Theoretical Operation of Solid Rod Cathodes

K. D. Goodfellow* and J. E. Polk*
Jet Propulsion Laboratory
California Institute of Technology
Pasadena, California

June 23, 1994

Abstract

Cathode erosion is one of the life limiting mechanisms for several classes of electric thrusters. Since cathode erosion is strongly dependent on the cathode temperature, a quantitative understanding of the effects of cathode operation on the cathode temperature is required. Comparisons between a newly developed two-dimensional and a previous quasi-two- dimensional model show excellent agreement. A radial pressure gradient is present across the tip of the cathode due to magnetic "pumping". This increased pressure can significantly affect both the magnitude and the radial distribution of the tip temperature profiles. Without the pressure effect the radial temperature profiles remain relatively flat and arc only slightly dependent on the current level. A comparison between the quasi-two-dimensional model and experimental data show excellent agreement for low current levels and only fair agreement at higher current levels.

Introduction

One of the major issues for the use of electric propulsion thrusters is lifetime. Missions analyses estimate that for electric propulsion to be a viable option, thruster lifetimes must be of the order of 1000 to 15,000 hours, Cathode erosion, one of the primary life-limiting mechanisms, has been shown to depend strongly on the cathode temperature [I]. Therefore, part of this study is intended to provide a simple means of predicting the cathode temperature for various thruster operating conditions. in addition, the thermal characteristics of the electrodes must be known to compute the overall thruster thermal loads to the spacecraft. This model also provides the appropriate boundary conditions at the cathode surface for models of the operating characteristics of the thruster. For example, the current contours within the magnetoplasmadynamic (MPD) thruster cannot be specified independently of the cathode temperature distribution because the majority of the current is from thermionic emission. Since the cathode model boundary conditions also depend on the characteristics of the main plasma, the two models must be ultimately coupled to obtain an overall model of the cathode region of the thruster.

Several different approaches have been taken in the past to characterize the nature of the hot-cathode arc physics [2,3,4,5] while others have focussed on the thermal model alone [6,7,8]. Past works have focussed primarily on one or the other of these models, but some combined models nave been presented [9,10,1 1,1 2]. That is, the plasma model provides the heat loads (boundary conditions) for the thermal model, and the

*Member of the Technical Staff

thermalmodel provides the surface temperature which strongly affects the plasma near the cathode through thermionic emission.

The thermal characteristics of cathodes in high-current gas discharges arc being investigated in a dedicated cathode test facility at the Jet Propulsion Laboratory (J PL). Axial temperature distributions and near-cathode plasma properties are being measured for various cathode designs as a function of current level, ambient gas pressure and flow rate. The objective of these experiments is to provide a databaseof measurements for comparison with theoretical predictions based on one-dimensional and two-dimensional heat transfer models of the solid cathode with radiation, convection and plasma sheath (arc attachment) boundary conditions. In this paper data obtained with a cylindrical thoriated-tungsten cathode in a discharge with flowing argon will be presented and compared with 1-D and 2-D cathode model predictions.

Cathode Model

The cathode model consists of two parts, namely a near-cathode plasma model and a thermal model of the cathode. The near-cathode plasma model connects the properties of the main plasma with the cathode. Specifically, given the plasma properties within a mean-free-path of the surface, the near-cathode model predicts the heat flux and current density to the cathode surface. With these boundary conditions and the traditional thermal transport mechanisms, the thermal model can predict the temperature distribution within the cathode. Because of the interdependency of the two models, they must be solved simultaneously.

Near-Cathode Plasma Model

An illustration of the near-cathode plasma is shown in Fig.(1). The Debye length, mean free path, and

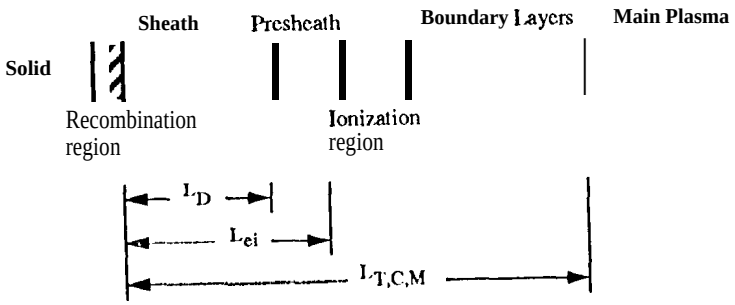

Figure 1: Near-cathode plasma regions.

thermal, concentration and momentum boundary layers arc represented by L_D, L_{ei} and $L_{T,C,M}$ respectively. For this study, only the surface, sheath, presheath and ionization regions arc modeled. In the main body of the plasma, the current is predominantly carried by the electrons, while in the sheath region the ion current may dominate. To match these regions an ionization region (which produces the required number of ions for the sheath region) is required between the sheath and the main plasma body. Similarly, a recombination

region exists at the cathode surface to produce a transition to pure electron conduction in the solid, At the surface, ions are also converted to neutrals, which then return to the plasma. A complete description of each region model, the overall near-cathode plasma model and sample solutions are given in Refs. [11] and [12].

In general the cathode surface is characterized by the material, the surface finish and the temperature. For this model, the recombination region is assumed to be infinitesimally thin and is considered as a surface effect. Incident particles from the sheath heat the surface while emitted particles cool the surface. The energy balance at the surface balances the energy deposited and removed by the particles with heat conduction into the solid, and radiative, convective and mass (surface erosion) transport to the surroundings, The surface heat flux is the net of the energy deposited from the incident ions and plasma electrons, and the energy removed by the thermionic electrons. The incident ions arc recombined and reemitted as neutrals.

For high cathode temperatures, thermionic emission is the dominant current conduction mechanism in the near-cathode region [10]. Thermionic emission is dcscribcd by the empirical Richardson-Dushman relation. In addition, the surface electric field acts to enhance the emission, a phenomenon known as the Schottky effect [13]. The magnitude of the electric field at the cathode surface is primarily determined by the characteristics of the sheath region.

The sheath region is assumed to contain collisionless particles with constant total energy (potential plus kinetic). Three species are considcrcd, namely monoenergetic thcrmionic (or beam) electrons, singly charged monoenergetic ions, and Maxwellian electrons originating in the plasma [2,4]. Further, the sheath thickness is assumed to be much less than the Larmor radii of the particles, and therefore, magnetic field effects on the particle trajectories are negligible.

For a stable sheath to occur, the ions must enter the sheath with energies equal to or greater than the Bohm minimum energy [14]. The ions here arc assumed to enter the sheath with energies equal to the Bohm minimum energy which is represented as the 1 Bohm potential. The plasma electrons are assumed to be Maxwellian and rcfercnccd to the electron density at the sheath edge. These electrons fall into two classes, namely those with sufficient kinetic energy to overcome the sheath retarding potential and reach the cathode surface and those with insufficient energy that arc repelled back to the main plasma. The corresponding flux of the high energy electrons constitutes the plasma electron current. The one-dimensional Poisson charge equation is used to describe the electric field and the electric potential

The ionization and presheath regions connect the sheath region with tile main plasma body [9] [13]. The purpose of the presheath region is to accelerate the ions so that they enter the sheath region with the minimum energy required for a stable sheath (Bohm energy) [14]. For this model the presheath region is combined with the ionization zone by requiring that ions leave the ionization region with the Bohm energy. The ionization region generates the required number of ion and electron pairs to match the sheath and main plasma body values. The number density of the electron and ion pairs that can be produced by ionization is determined by the energy balance. Since only singly charged ions arc considcrcd, the production rates of the ions and the electrons are equal.

'J'here arc upper and lower limits on the number of ion/electron pairs in the ionization region. The upper limit on the number of possible ions produced is set by the pressure assuming fully ionized plasma. If this limit is reached, the excess energy to the ionization region is assumed to be dissipated in modes other than ionization or thermal energy. Similarly, if the plasma is sufficiently ionized already, then a minimum number of ions exist. That is, ion/electron pairs produced outside of the ionization region arc used. The ionization fraction represents the number of ions per heavy particle (ions plus neutrals). The values for the pressure and the ionization fraction only affect these limiting conditions and have no effect if the number of ions produced is governed by the energy balance. in other words, if the number density calculated by the energy balance is lower than the minimum value set by the ionization fraction then the value set by the ionization fraction is used. Similarly, if the number density value from the energy balance is greater than the value set by the pressure, the value calculated from the pressure is used.

Magnetic Pressure Effects

A radial pressure gradient is present across the tip of the cathode due to magnetic "pumping". The interaction of the axial current with the induced azimuthal magnetic field produces a inward radial body force on the plasma. This force must be counter acted by an increase in pressure to maintain equilibrium. Maxwell's V x $\vec{B}$ provides the relation for the purely azimuthal magnetic field given by

$$B_\phi = \frac{\mu_o I_{\text{enc}}}{2\pi r} \tag{1}$$

where lent is the enclosed current and r is the radial position, The balance between the magnetic "pumping" and the pressure is given by

$$j_z B_\phi = -\frac{dP}{dr} \tag{2}$$

where j_z is the axial current density. For the special case of constant current density where $I_{\text{tot}} = j_z \pi r^2$, Eq. (2) can reintegrated to provide

$$P = P_o + \frac{\mu_o j_z^2 r_c^2}{4}\left(1 - \frac{r}{r_c}\right) = P_o + \frac{\mu_o I_{\text{tot}}^2}{4\pi^2 r_c^2}\left(1 - \frac{r}{r_c}\right) \tag{3}$$

where PO is the pressure at the outer edge of the cathode and r_c is the cathode radius[15]. To determine the average pressure across the cathode tip segment, Eq. (3) is evaluated at

$$r = \sqrt{\frac{r_i^2 + r_o^2}{2}} \tag{4}$$

where r_i and r_o are the inner and outer radii respectively. At this radial location the inner and outer areas arc equal. For the case where $r_i = 0$, Eq.(3) becomes

$$P = P_o + \frac{\mu_o j_z^2 r_c^2}{8} = P_o + \frac{\mu_o I_{\text{tot}}^2}{8\pi^2 r_c^2}. \tag{5}$$

Tbc tip pressure is therefore dependent on both the current (or current density), and the tip area. For a given geometry the quadratic increase in pressure with current can significantly change the arc attachment characteristics. Comparisons of solu tions with and without, the magnetic pressure effect are presented later.

For the case where the current density is not constant across the tip, a different approach is required. The tip of the cathode can be discretized into a series of concentric rings with a constant current density for each ring. Equation 2 can be integrated for a ring segment to provide

$$P_i = P_o + \frac{\mu_o j_{z,o}}{2\pi}\left[\frac{\pi j_{z,o}}{2}\left(r_o^2 - r_i^2\right) + \left(I_i - j_{z,i}\pi r_i^2\right)\ln\left(\frac{r_o}{r_i}\right)\right] \tag{6}$$

where I_i is the enclosed current up to the inner radius. The second term is the correction for the nonuniform current density.

Overall Near-Cktl~odc Plasma Model

The surface, sheath and presheath/ionization region models arc combined to form the overall near-cat hode plasma model, The heat flux and the current density to the surface arc determined for values of the electron temperature, the cathode temperature, the sheath voltage, the pressure, the ionization fraction, the surface material, and the gas type.

The relative values of the ion and plasma electron current arc predominantly determined by the sheath voltage. 'l'he heat flux to the cathode surface increases until the maximum ion number density, which is set by the pressure in the ionization region, is reached, and then decreases. For cathode temperatures below the peak, ion and plasma electron heating dominate, while for values above the peak the ion and plasma electron heat fluxes are approximately constant. Therefore, the total heat flux decreases because the thermionic electron cooling effect begins to dominate. It is this set of curves that forms the boundary conditions for the thermal model. The near-cathode plasma model is most sensitive to the material work function as expected duc to the exponential nature of the Richardson-Dushman equation.

Thermal Model

For a given set of boundary conditions, the thermal model describes the temperature distribution within the cathode. There arc several orders of approximation by which the thermal model can be done ranging from simple one-dimensional analytical models [16] to complex two-dimensional (axisymmetric) numerical ones. A quasi-two-dimensional numerical solution for a cathode which includes radial radiation and convection, and ohmic heating, for a cylindrical rod with a conical tip is presented in Ref. [12]. While the simple models do not have the capabilities for solving the problems of interest, they provide useful insights into the solution trends and provide good first approximations for the starting conditions for the more advanced models.

Two-Dimensional Axisymmetric Finite Difference Thermal Model

Experimental data suggest that for MPD thrusters the arc attachment may be over a significant, portion of the exposed surface area [I]. Therefore, the thermal model must be capable of modeling ohmic heating and arc attachment over a range of axial positions as well as the tip. Experimental evidence shows that the cathode centerline temperatures significantly excced the outer temperatures for some operating conditions. The arcjet thruster cathode tip craters have been observed, indicating that melting has occurred on the centerline [17]. Internal ruptures have also been observed in MPD thruster cathodes [1 6].

This mode] is capable of variable geometries, temperature-dependent material properties, and multimode heat transfer (arc attachment plus radiative and convective transport) at any axial location. Energy and current balances arc performed on each cell for the two-dimensional model using a finite volume technique.

The energy balance for each cell, as shown in Fig. (2), is given by:

$$q_{i-1,j} + q_{i+1,j} + q_{i,j-1} + q_{i,j+1} + q''' Vol = 0 \tag{7}$$

where

$$q''' = \frac{I^2 R}{dz} \tag{8}$$

is the heat generated per unit length by Ohmic heating, vol is the cell volume, and dz *is* the cell length. The resistance, R, is given by

$$R = \rho_e dz / A_c \tag{9}$$

where ρ_e is the electrical resistivity and A_c *is* the cell cross-sectional area. The axial heat load, calculated at the cell wall, is given by

$$q_{i+1} = q''_{i+1} A_{i+1} \simeq k_{th,i+1} A_{i+1} \frac{T_{i+1} - T_i}{dz} \tag{10}$$

where k_{th} is the thermal conductivity. The temperature gradient has been discretized using the central differencing technique with a discretization error of the order of $(dz/2)^2$ [?]. Since the cell wall temperature is not needed to calculate the heat flux, this technique effectively doubles the number of grid cells used. That

Figure 2: Energy inputs for the two-dimensional thermal model.

is, half of the number of cells are required to achieve the same spatial resolution as a direct discretization of tbe differential equations. Using Eq. (10) for the four wall heat fluxes, Eq. (7) can then be rewritten as

$$\frac{k_{th,i-1,j}A_{i-1,j}}{dz}T_{i-1,j} + \frac{k_{th,i+1,j}A_{i+1,j}}{dz}T_{i+1,j} + \frac{k_{th,i,j-1}A_{i,j-1}}{dr}T_{i,j-1} + \frac{k_{th,i,j+1}A_{i,j+1}}{dr}T_{i,j+1} - CT_i + q'''Vol = 0 \quad (11)$$

where

$$C \equiv \frac{k_{th,i-1,j}A_{i-1,j}}{dz} + \frac{k_{th,i+1,j}A_{i+1,j}}{dz} + \frac{k_{th,i,j-1}A_{i,j-1}}{dr} + \frac{k_{th,i,j+1}A_{i,j+1}}{dr} \quad (12)$$

For the method of Successive Over Relaxation (SO R), Eq. (1 1) is rewritten as

$$T_{i,j}^{k+1} = T_{i,j}^{k} + \frac{w}{C}\left(\frac{k_{th,i-1,j}A_{i-1,j}}{dz}T_{i-1,j} + \frac{k_{th,i+1,j}A_{i+1,j}}{dz}T_{i+1,j} + \frac{k_{th,i,j-1}A_{i,j-1}}{dr}T_{i,j-1} + \frac{k_{th,i,j+1}A_{i,j+1}}{dr}T_{i,j+1} - CT_i + q'''Vol\right). \quad (13)$$

The heat loads for the exterior cells are determined from the plasma model. The temperature value at tbc "kth" time-step is T_i^k, T_i^{k+1} is the value at the next time-step, and w is tbe relaxation coefficient. If w is less than one the calculation is "under-relaxecl" while if w is greater t, ban onc tbe calculation is "over-relaxed" [?]. An iteration is performed until the temperature change between consecutive time steps is within the specified tolerance and the global energy balance is within a specified tolerance. Over-relaxation will generally make the solution converge more quickly by taking larger steps but may also make the calculation diverge. The computer program is setup to automatically decrease the relaxation coefficient if the calculation diverges more than a specified number of consecutive steps. This technique has proven to be very useful in maintaining code stability.

Current conservation is considered for the group of cells at each axial position. The total current for each group is given by

$$I_{\text{tot}} = \sum_{i=1}^{n} j_i A_{c,i} + j_{ro} A_{ro} + j_{ri} A_{ri} \tag{14}$$

where n is the number of radial cells. The current is distributed amongst the cells within the group by considering the cells as a parallel resistor network where the resistance for each cell is given by Eq. (9). The current for each cell is given by Ii = V/R_i where V is the voltage drop across the group. The voltage drop is determined by, $V = I_{\text{tot}} R_{\text{tot}}$ where R_{tot} is the total resistance for the parallel network, and I_{tot} is the current leaving the cell (towards the cathode base). This current value is used to calculated the Ohmic heating within the cell. For cells with radial current inputs, this will over-predict the amount of Ohmic heating. However, for a sufficiently fine grid spacing, this is effect negligible.

The nonlinearities of the thermal equations larger temperature gradients in the tip region than in the base region. To increase the accuracy of the discretization without increasing the number of cells and correspondingly increasing the solution time, the cells arc '(packed" towards the tip, An algebraic grid generator that allows the minimum grid spacing to be placed anywhere along the cathode. The transformation consists of two third order polynomials [19].

Combined Thermal and Plasma Model Solutions

The near-cathoclc plasma model and the cathode thermal model are cornbincd to form an overall model of the cathode-plasma interaction. Figure (3) shows the heat flux and surface temperature relations for both the near-cathode plasma model and the simple heat transfer model (tungsten rod with a 12 mm diameter and a 65 mm length). Solutions exist at three points; namely, at the origin (trivial solution) and the two nonzero solutions where the curves intersect. Of these, only the high temperature (fully ionized) solution is numerically stable. Therefore, the value of the pressure is important for this type of discharge and the energy balance in the ionization region is not needed.

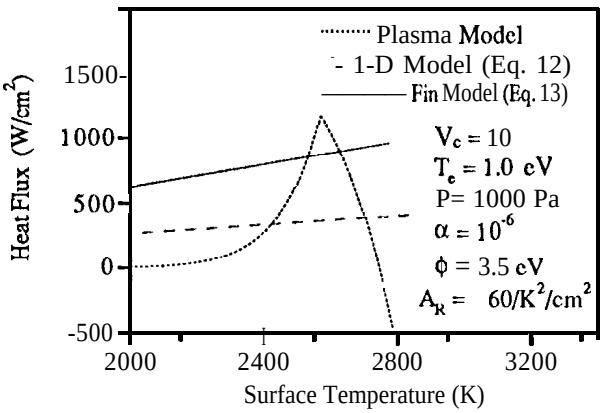

Figure 3: Heat flux as function of surface temperature with thermal model solutions.

For the special case where the arc only attaches at the tip a series of solutions can be reasonably determined. For a given set of thermal characteristics for the one-dimensional model, and given the plasma properties, one can solve for the intercept point of the one-dimensional thermal model and near-cathoclc

plasma mode] for the fully ionized (stable) case. For example, consider the case of zero heat flux to the surface from the plasma. This special case does not depend on the type of thermal model or on the thermal model parameters, and therefore provides a good reference point for examining the plasma effects. The inclusion of the magnetic pressure effect can have a significant affect on the arc characteristics. Figure 4 shows that for a given sheath voltage and current level, the magnetic pressure effect increases the cathode tip temperature. Since the magnetic pressure effect increases with current level, the tip temperature also increases with current level. 'I'he magnetic "pumping" is forcing the arc into a smaller attachment area. The current density must therefore increase, which results in an increase in tip temperature because thermionic emission is the dominant mode. Plots of attachment area as a function of sheath voltage can be seen in Fig. (5), and as a function of tip temperature in Fig. (6). For these test cases the plasma heat flux to the

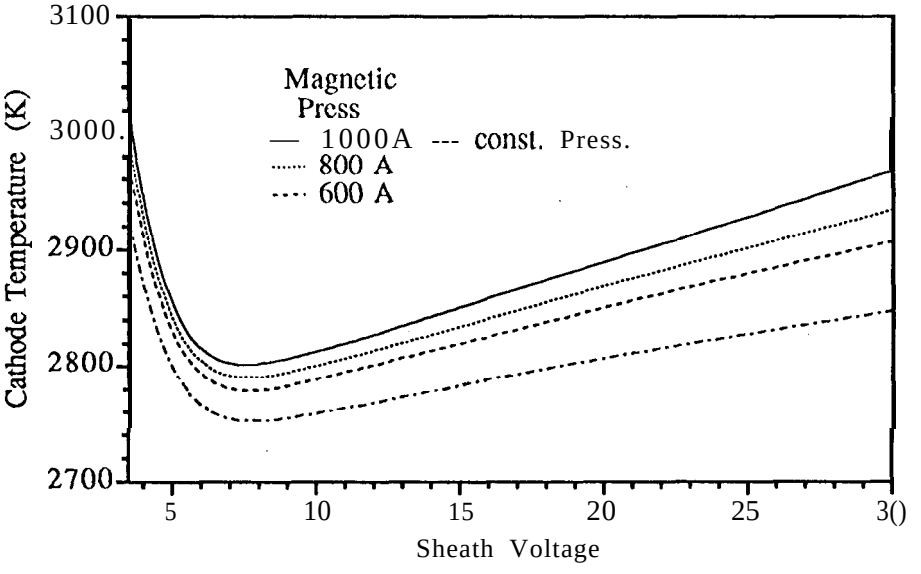

Figure 4: Cathode temperature as a function of sheath voltage with current as a parameter

surface was set to zero, the material work function was 3.2 eV, the electron temperature was 1.0 cV, the static pressure was 3000 Pa, and the sheath voltage was 8 volts. As the sheath voltage drops from a high value, the cathode temperature decreases because the ion energy transferred to the surface is decreasing. The decrease in temperature produces a comparable decrease in thermionic current. Therefore the attachment area must increase to maintain the same total current since j_i and j_t arc both decreasing. The minimum in temperature corresponds to the maximum in attachment area. As the voltage is further decreased the temperature begins to increase as the plasma electron heating becomes important. Even though the plasma electron current is increasing, the thermionic current is increasing faster and therefore the attachment area decreases. For a given tip temperature, two attachment area values may be possible corresponding to two different sheath voltages. The smaller attachment area will have the larger sheath voltage. Also, for a given attachment area, two temperature solutions may be possible with the smaller temperature corresponding to the larger voltage.

A series of test cases were performed to compare the two-dimension al and quasi-two-dimensional models with and without the magnetic pressure effect. The results arc shown in 'l'able (1). The quasi-two-dimensional

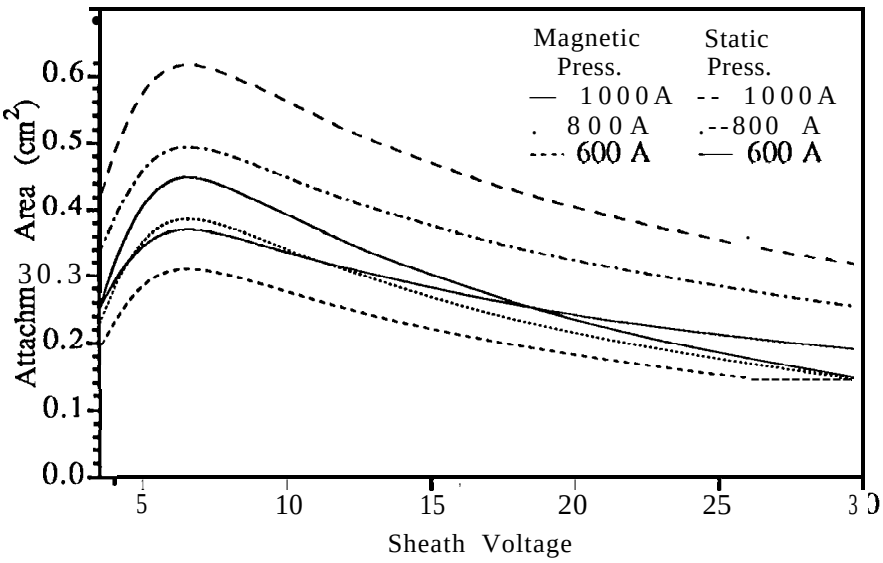

Figure 5: Arc attachment area as a function of sheath voltage with current as a parameter.

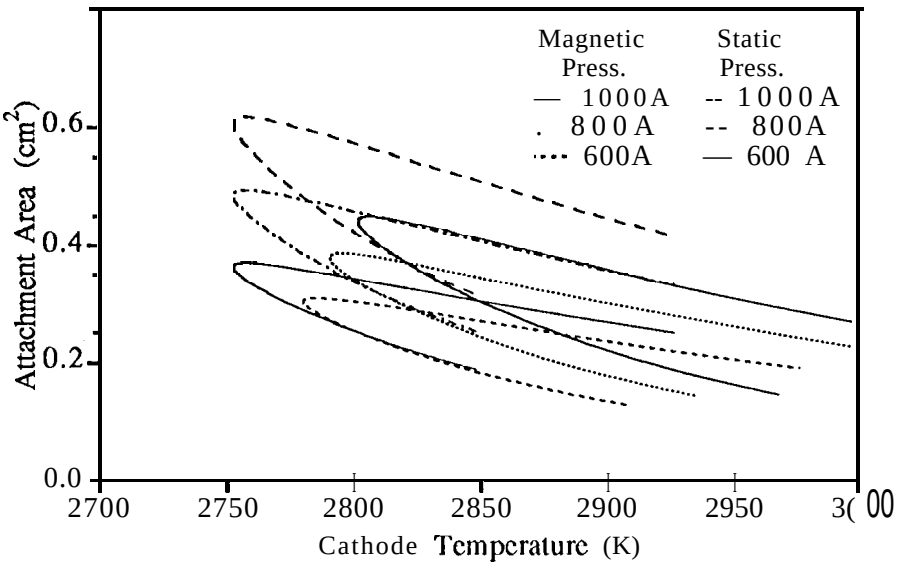

Figure 6: Arc attachment area as a function of cathode temperature with current as a parameter.

cases were performed using a cathode length of 65 mm and a fixed base temperature of 1500 K. The cylindrical rod shape with a radius of 4.17 mm and a flat tip was used for all of the cases. The radial emissivity was 0.4 with a environmental temperature of 500 K. The pressures reported in the table for the two-dimensional cases arc the centerline pressure while the pressures for the qua.ii-two-dimensional cases the table value is the average pressure. The tip pressure gradient was assumed to result from a plasma density gradient, and the electron temperature was assumed to bc constant at 1 eV. The two-dimensional cases were performed with a shorter cathode length to decrease the the number of cells and therefore decrease the computational time. A length of 18.86 mm corresponding to a length to diameter ratio of 4. The base temperature for these cases was set to the value calculated for the same position using the quasi-two-dimensional model.

The two models agree reasonably well. The att achment areas arc comparable and the tip temperature for the quasi-two-dimensional model is c1osc to the average value for the two-dimensional mode]. The quasi-two-d irnensional model therefore provides a good first order approximation. Since the computational time required for the quasi-two-dimensional solutions is significantly less than for the full two-dimensional model (minutes verses hours), it may bc effectively used to explore the effects of different parameters. Then the two-dimensional model can be used to get a detailed description for specific conditions.

Current (A)	Area (cm^2)	P (] 'a)	T_{cent} (]{)	T_{edge} (K)	q_{tip} (W)
Two-Dimensional					
Magnetic Press.					
600	0.366	4086	2705	2552	372
800	0.445	4565	2727	2604	348
1000	0.496	5347	2758	2637	317
Static Press.					
600	0.430	3000	2663	2567	397
800	0.550	3000	2670	2620	368
1000	0.660	3000	2675	2659	331
Quasi-two-Dimensional					
Magnetic Press.					
600	0.378	3476	2732		827
800	0.446	3717	2754		651
1000	0.497	4005	2774		518
Static Press.					
600	0.439	3000	2710		722
800	0.553	3000	2722		526
1000	0.664	3000	2731		382

Table 1: Two-dimensional and quasi-two-dimensional model comparison results.

A comparison of the tip radial temperature profiles arc shown in Fig. (7). For the static pressure cases, the temperature dots not change significantly for different current levels or radially across the attachment area.. Outside the attachment area the temperature decreases more rapidly duc to radial cooling. The addition of the magnetic pressure effect results in a increase in the temperature and a corresponding decrease in the attachment area for a specific current level. The radial decrease in the temperature profiles with the magnetic pressure is primarily duc to the radial change in pressure. The heat flux and current density are sensitive to the pressure values in the plasma model for the fully ionized solution [1 1]. The peak temperature for these plasma conditions is about 2600 K. The temperatures within the attachment area for all of these cases arc above this value and therefore, all of these solutions arc on the fully ionized side of the curve [1 1,12].

Temperature contour plots for the two-d imensional model with the magnetic pressure effect are shown in

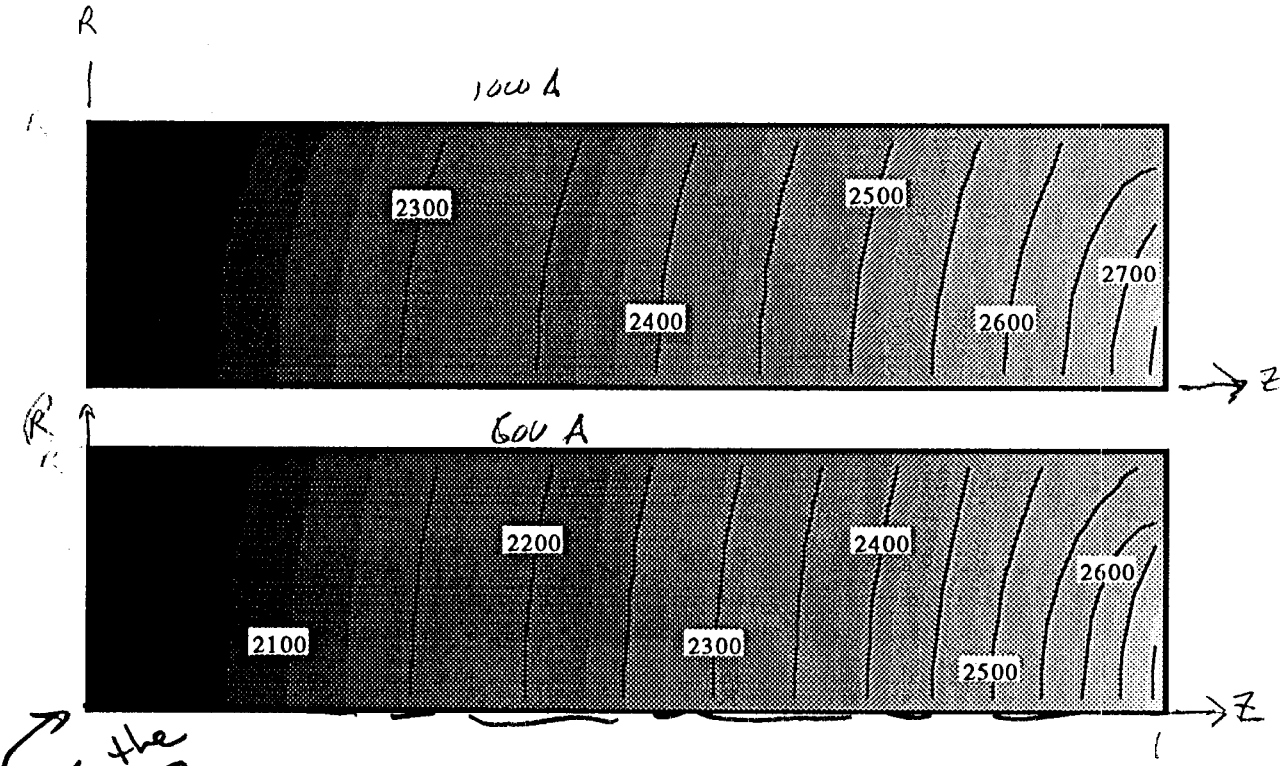

is this the cathode centerline?

The geometry of this plot is not clear

Fig 8

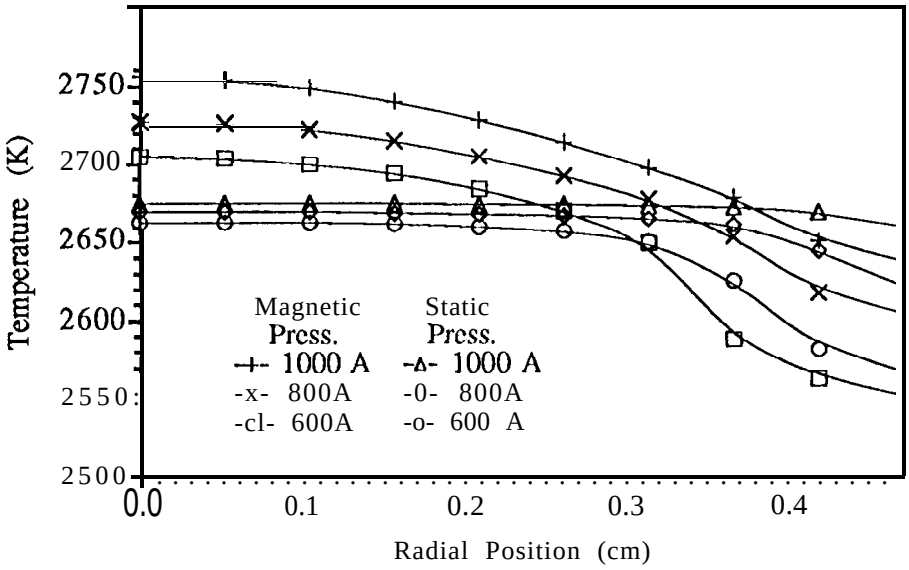

Figure 7: Radial tip temperature distributions.

Figure 8: Cathode temperature contours.

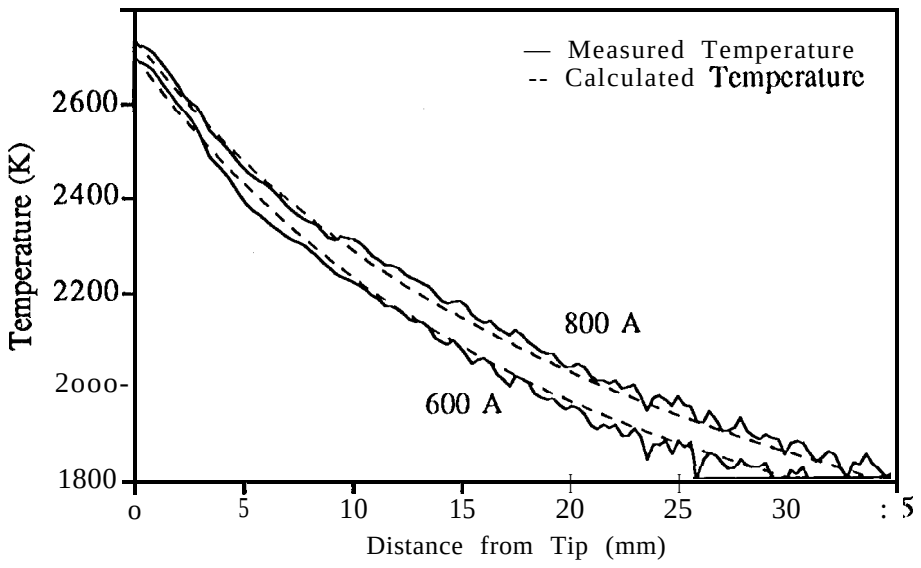

Figure 9: Measured and calculated axial temperature profiles for low currents.

Fig. (8) for current levels of 600 and 1000 A. The contour shapes are similar for both current levels except right at the tip. The sharp bend in the 2650 K line in the 600 A case and the 2600 K line in the 1000 A case show the edges of the attachment areas. For these conditions, Ohmic heating provides 15 percent of the total input heat for the 600 A case, and 38 percent, of the total input heat for the 1000 A case.

Comparison with experiments

Experiments to validate the model were performed in the JPL cathode test facility (CTF)[20,21]. Cathode axial temperature distributions were measured as a function of time at current levels ranging from 600 to 1400 A and an argon mass flow rate of 0.75 g/s for two discharge chamber pressure levels, 2800 Pa (21 Torr) and]470 Pa (1 1 Torr). The temperature as a function of axial distance from the tip measured at 2800 Pa is displayed in Figures (9) and (10).

The characteristic shape of temperature profiles measured at 1470 Pa is considerably different from that observed at the higher pressure [20]. A small temperature peak at the tip is followed by either a plateau in temperature or a second peak located further upstream. The base temperature and the temperature along the cathode shaft rise much more dramatically with current. This behavior suggests that a transition between tip attachment and a more diffuse arc attachment triggered by a decrease in pressure is occurring.

Post-test examination of the thoriated-tungsten cathode shows that some process results in a rapid accumulation of thorium on the cathode tip. A possible explanation is that thorium metal evaporated from the cathode is ionized in the discharge and drawn back to the tip by the electric field in the column.

Comparison of Measured and Calculated Temperature Distributions

The model parameters were selected from the best data approximations available. The ambient pressure, emittance, convection coefficient and the Richardson coefficient for thermionic emission were fixed at 2800 Pa,

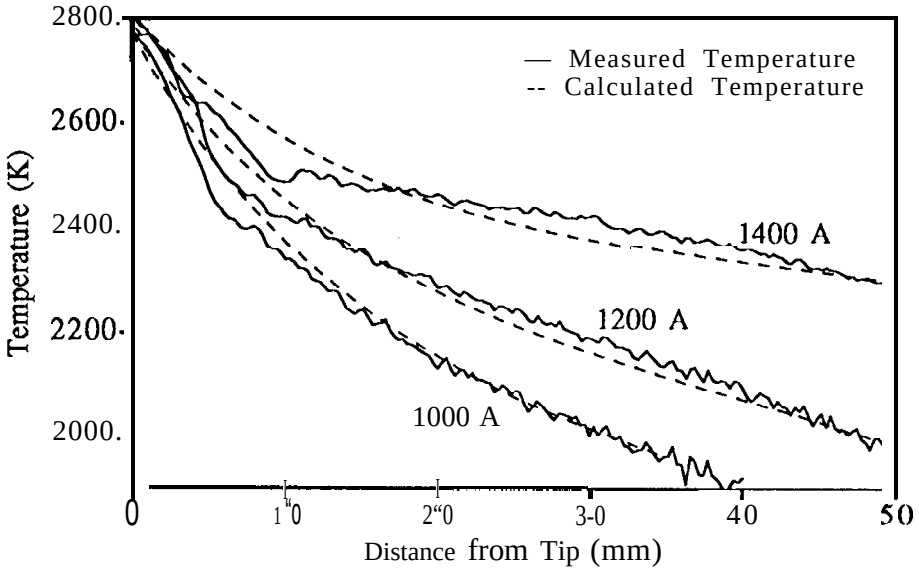

Figure 10: Measured and calculated axial temperature profiles for high currents.

0.4, 0.O, and 60 A/cm^{2}K^2, respectively. Previous studies indicated that a temperature minimum occurs for a sheath voltage of 7–8 V, so a value of 8 V was used in this study [12]. For the comparison with measured profiles, the upstream temperature boundary condition was set equal to the measured temperature at a particular location on the shaft. The work function was then varied to match the measured tip temperature, The input and calculated model parameters are shown in 'l'able (2) and the calculated temperature profiles are plotted in Figures (9) and (10).

The calculated temperature profiles agree remarkably well with the measured distributions for currents of 600 and 800 A, indicating that in this range the temperature can bc adequately described by tip attachment and radiative cooling. For higher current levels, however, the calculated profiles do not match the measured profiles as well. The observed luminosity profiles in this current range can be interpreted either as having

Parameter	Case 1	Case 2	Case 3	Case 4	Case 5
Current (A)	1400	1200	1000	800	600
Work Function (eV)	3.22	3.20	3.22	3.20	3.18
Tip Temperature (K)	2811	2778	2772	2738	2703
Current Density (A/cm^2)	2276	2047	1809	1629	1458
Attachment Area (cm^2)	0.615	0.586	0.553	0.491	0.412
Tip Pressure (Pa)	4393	4028	3704	3451	3237
Effective Work Function (eV)	3.005	2.990	3.014	2.997	2.981

Table 2: Model parameters used in the comparison with measured temperature profiles.

an unusually bright tip or a slightly darker band extending from 5 to 10 mm behind the tip. A dark band might bc explained by a region of somewhat lower emittance. A brighter tip could result from a higher

emittance due to thorium oxide layers or surface roughness or a true temperature peak due to a more complex arc attachment or thermal choking in the hemispherical portion of the tip. The slightly convex form of the measured temperature profiles along the shaft could be due to more resistive heating than the model calculates or convective cooling by the cold gas injected at the base, which may play a more important role at high currents where the base temperature is nigher.

The mode] indicates that the work function is approximately constant at 3.2 eV and that increases in current are accommodated by an increase in the current density and the attachment area. This value of the work function agrees well with that for bulk thorium on tungsten, which is consistent with the observations of thorium accumulation on the tip. For all five cases the calculated attachment area is less than the cross-sectional area of the cylinder, so the modeling assumption of tip attachment is internally consistent, The model also shows that magnetic pinching can substantially increase the average tip pressure and that the Schottky effect reduces the work function by about 0.2 eV. The fact that the model input values required to match the observed tip temperatures and the calculated output variables are reasonable lends confidence to the model. However, a number of additional experiments are required to verify these parameters.

Conclusions

Comparisons between the two-dimensional and quasi-two-dimensional models show excellent agreement. The quasi-two-dimensional model provides a good first approximation to the cathode operating characteristics when the arc is attached only at the tip. The increased pressure resulting from the magnetic pressure effect can significantly affect both the magnitude and the radial distribution of the tip temperature profiles. Without the pressure effect the radial temperature profiles remain relatively flat and are slightly dependent on the current level. A comparison between the quasi-two-dimensional model and experimental data show excellent agreement for low current levels and only fair agreement at higher current levels. It is not certain at this time whether this disagreement is due to errors with the model or due to errors with the temperature measurements.

Acknowledgements

The research described in this paper was conducted at the Jet Propulsion Laboratory, California Institute of Technology under contract with the National Aeronautics and Space Administration.

References

[1] J. E. Polk, A. J. Kelly, and R. G. Jahn. Mechanisms of Hot Cathode Erosion in MPD Thrusters. In 21*' *International Electric* Propulsion *Conference*, Orlando, FL, 1990. AIAA-90-2673.

[2] P. D. Prewett and J. E. Allen. The Double Sheath Associated with a Hot Cathode. Proceedings *of the Royal Society of London,* 348:435–446, 1976.

[3] D. E. Siegfried and P. J. Wilbur. A Model for Mercury Orificed Hollow Cathodes: Theory and Experiment. *AIAA Journal,* 22(10):1405–1412, 1984.

[4] K. D. Goodfellow and S. N. B. Murthy. Electrode l'recesses and MPD Thruster Operation. In 24th *Joint* Propulsion Conference, Boston, MA, 1988. AI AA-88-3207.

[5] A. Salhi and P. J. Turchi. A First-Principles Model for Orificed Hollow Cathode Operation. In 28^{th} *Joint Propulsion Conference,* Nashville, TN, 1992. AIAA 92-3742.

[6] 1{. Kuwahara and ct. al. Thermal Characteristics of MPD Arcjet. in 17^{th} *International Electric Propulsion Conference,* Tokyo, Japan, 1984. IEPC 84-59.

[7] R. C. Mehta. Thermal Analysis of a Conical Cathode of an MPD Arc. *AIAA Journal*, 17(11):1272–1274, 1979.

[8] 'J'. Weng and E. J. Seldin. Calculation of Steady State Temperatures in Graphite electrodes in an Electric Arc Steel Furnace. *Carbon*, 15:391-398, 1977.

[9] W. L. Bade and J. M. Yes. A rcjct Technology Research and Development-Final Report. Technical Report NASA CR-54687, AVCO Corporation, Wilmington, MA, 1965.

[10] D. Q. King. Feasibility of Steady-State Multi-Megawatt MPD Thrusters. In 18^{th} *International Electric Propulsion Conference*, Alexandria, VA, 1985. AIAA 85-2004.

[11] K. D. Goodfellow, T. J. Pivirotto, and J. E. Polk. Applied-Field Magnetoplasmd ynamic Engine Developments. In 28^{th} *Joint Propulsion Conference*, Nashville, TN, 1992. AIAA 92-3293.

[12] K. 1). Goodfellow and J. E. Polk. High Current Cathode Thermal Behavior, Part I: Theory. In 23^{rd} "*International* Electric *Propulsion Conference,* Seattle, WA, 1993. IEPC 93-030.

[13] W. Neumann. *The Mechanism of the Thermoemitting Arc Cathode.* Akademic-Verlag Press, Berlin, Germany, 1987.

[14] D. Bohm. *The Characteristics of Electrical Discharges in Magnetic Plasma.* McGraw-Hill, Ncw York, 1949.

[15] R. G. Jahn. The *Physics of Electric Propulsion,* McGraw-Hill, New York, 1968.

[16] F. P. Incropera and D. P. DeWitt. *Fundamentals of Heat Transfer.* John Wiley and Sons, New Yolk, 1981.

[17] W. D. Deininger, A. Chopra, K. D. Goodfellow, and J. W. Barnett. Cathode Erosion Test for 30 kW Arcjets. In 25^{th} *Joint Propulsion Conferen ce,* Monterey, CA, 1989. AIAA 89-2264.

[18] M. Auweter-Kurtz and et. al. Cathode Phenomena in Plasma Thrusters. In 21^{st} *international Electric Propulsion Conference,* Orlando, FL, 1990. AIAA 90-2662.

[19] J. D. Hoffman, May 1994. Personal communication.

[20] J. E. Polk and K. D. Goodfellow. High Current Cathode Thermal Behavior, Part 11: Experiments. In 23"d *international Electric Propulsion Conference*, Seattle, WA, 1993. IEPC 93-029.

[21] J. E. Polk and K. D. Goodfellow. Experimental Investigation of Solid Rod Cathode Operation. in 30^{th} *Joint Propulsion Conference,* Indianapolis, IN, 1994. AIAA 94-3)31.